

Pointwise Temporal Decay of Solutions of the Klein-Gordon Equation in Schwarzschild Spacetime

Elliott Fairchild

Under the direction of

Ethan Sussman
Massachusetts Institute of Technology

Research Science Institute

July 17, 2020

Abstract

We investigate the time asymptotics of solutions of the free Klein-Gordon equation in Minkowski and Schwarzschild background spaces. We provide analytical methods to show that a $t^{-3/2}$ growth law holds in solutions of the equation over Minkowski spacetime and describe numerical methods that attempt to extend this law to radially symmetric solutions of the equation over Schwarzschild spacetime. We describe and explain examples where these methods fail to apply.

Summary

There is a mathematical equation that models important systems in areas of physics like quantum mechanics and general relativity. We wish to examine this equation to determine how these systems evolve over time. A previous result shows that these systems are governed by functions that decay over time, if the systems are set up in flat space. We attempt to determine how the corresponding functions evolve over time if the systems are instead set up in a special example of curved space.

1 Introduction

In 1926, Austrian-Irish physicist Erwin Schrödinger [1] computed the spectral series for hydrogen by considering the hydrogen atom's electron as a wave $\psi(t, x)$ moving in a potential well V created by the proton. In doing this, Schrödinger arrived at the now famously known Schrödinger equation

$$i\hbar \frac{d}{dt} |\psi(t)\rangle = \hat{H} |\psi(t)\rangle,$$

where \hbar is Planck's constant, $|\psi(t)\rangle$ represents the continuous one parameter unitary group of rays $\psi(x)$ on a Hilbert space \mathcal{H} , and \hat{H} is the corresponding infinitesimal generator of the group [2].

While the Schrödinger equation was found to extend to a number of quantum mechanical systems, it was also found to suffer from being inconsistent with special relativity [3]. In an attempt to bridge the gap between special relativity and the Schrödinger equation, Oskar Klein and Walter Gordon [4] derived the equation

$$\left(\frac{1}{c^2} \frac{\partial^2}{\partial t^2} - \Delta + \frac{m^2 c^2}{\hbar^2} \right) \psi = 0 \tag{1}$$

where c is the speed of light, ψ is the system's wave function, m is the mass parameter, and Δ is the negative definite Laplacian. The result is the free Klein-Gordon equation in a Minkowski (flat) background space, which complies with special relativity and governs the motion of one particle states.

Because ψ is a function of time and space, it is reasonable to examine the evolution of ψ in time. In this case, it has been shown that solutions of equation (1) decay pointwise like $t^{-3/2}$ as $t \rightarrow \infty$ [5]. However, it has been conjectured by Burko [6] that when the background space has been changed to Schwarzschild spacetime, a model for the gravitational field outside a black hole, solutions of the corresponding free Klein-Gordon equation behave like $t^{-5/6}$ asymptotically. If this conjecture were true, techniques applied to understanding fundamental questions of systems in Minkowski spacetime would prove irrelevant to the Schwarzschild

case. It is thus of interest to understand precisely the asymptotics of solutions of the Klein-Gordon equation in Schwarzschild spacetime. In this paper, we describe numerical methods we used to calculate spherically symmetric solutions of the free Klein-Gordon equation in Schwarzschild spacetime in an attempt to better understand their temporal decay. In sections 2 and 3, we provide previous results essential to our question. In section 4, we describe our main numerical methods and results.

2 Preliminaries

In this section we review classical results from mathematical physics and partial differential equations, particularly focusing on asymptotic methods for evaluating oscillatory integrals. Throughout the paper, we assume familiarity with fundamental notions of functional analysis and Riemannian geometry —multiindex notation, the Japanese bracket, Fréchet spaces, Riemannian and Lorentzian manifolds, metric tensors, and Hessians — and their standard notations. For a detailed introduction to these topics, we refer the reader to Reed and Simon [2] and Do Carmo [7].

Schwartz Functions and Tempered Distributions

Definition 2.1. Let $C^\infty(\mathbb{R}^n)$ be the space of smooth complex-valued functions on \mathbb{R}^n . The space $\mathcal{S}(\mathbb{R}^n)$ of *Schwartz functions* consists of all $\phi \in C^\infty(\mathbb{R}^n)$ such that for all $k \in \mathbb{N}_0$, we have

$$\|\phi\|_k = \sup_{\substack{x \in \mathbb{R}^n \\ |\alpha|+|\beta| \leq k}} |x^\alpha D^\beta \phi(x)| < \infty.$$

Remark. With the seminorms $\|\phi\|_k$, we see that $\mathcal{S}(\mathbb{R}^n)$ is a Fréchet space.

The space $\mathcal{S}(\mathbb{R}^n)$ being a topological vector space, we now define its dual $\mathcal{S}'(\mathbb{R}^n)$, the space of tempered distributions.

Definition 2.2. The space $\mathcal{S}'(\mathbb{R}^n)$ of *tempered distributions* is the space of continuous linear functionals $u : \mathcal{S}(\mathbb{R}^n) \rightarrow \mathbb{C}$. It is equipped with the weak topology and has seminorms $|u|_\phi = |u(\phi)|$ for $\phi \in \mathcal{S}(\mathbb{R}^n)$.

There is a natural map $\mathcal{S}(\mathbb{R}^n) \ni \phi \mapsto T_\phi \in \mathcal{S}'(\mathbb{R}^n)$ given by $T_\phi(\psi) = \int_{\mathbb{R}^n} \phi(x)\psi(x) dx$ for $\psi \in \mathcal{S}(\mathbb{R}^n)$.

Proposition 2.1. $\phi \mapsto T_\phi$ is continuous, injective, and has dense range.

While the above proposition follows fairly directly from the definition of T_ϕ , we refer the reader to [2] for a rigorous proof.

Fourier Transform

As wave equations primarily involve differential operators, it is of use to describe a tool that translates partial differential equations to ordinary differential equations.

Definition 2.3. We define the Fourier transform \mathcal{F} of $\phi \in \mathcal{S}(\mathbb{R}^n)$ by

$$(\mathcal{F}\phi)(\xi) = \hat{\phi}(\xi) = \int_{\mathbb{R}^n} e^{-ix\xi} \phi(x) dx, \quad \xi \in \mathbb{R}^n,$$

and the inverse Fourier transform of $\psi \in \mathcal{S}(\mathbb{R}^n)$ by

$$(\mathcal{F}^{-1}\psi)(x) = (2\pi)^{-n} \int_{\mathbb{R}^n} e^{ix\xi} \psi(\xi) d\xi, \quad x \in \mathbb{R}^n.$$

One of the more useful properties of the Fourier transform is its ability to translate between multiplication and differentiation. We state the result here, but refer the reader to [2] for its proof.

Proposition 2.2. *We have*

$$\begin{aligned} \mathcal{F}(D_{x_j}\phi) &= \xi_j \mathcal{F}\phi, & \mathcal{F}(x_j\phi) &= -D_{\xi_j} \mathcal{F}\phi, \\ \mathcal{F}^{-1}(D_{\xi_j}\phi) &= -x_j \mathcal{F}^{-1}\phi, & \mathcal{F}^{-1}(\xi_j\phi) &= D_{x_j} \mathcal{F}^{-1}\phi, \end{aligned}$$

and $\mathcal{F}, \mathcal{F}^{-1} : \mathcal{S}(\mathbb{R}^n) \rightarrow \mathcal{S}(\mathbb{R}^n)$.

Remark. From Proposition 2.2, we have that for $\phi, \psi \in \mathcal{S}(\mathbb{R}^n)$,

$$T_{\mathcal{F}\phi}(\psi) = \int_{\mathbb{R}^n} \int_{\mathbb{R}^n} e^{ix\xi} \phi(x) dx \psi(\xi) d\xi = \int_{\mathbb{R}^n} \int_{\mathbb{R}^n} \psi(\xi) e^{ix\xi} d\xi \phi(x) dx = T_{\phi}(\mathcal{F}\psi)$$

which allows us to extend $\mathcal{F}, \mathcal{F}^{-1}$ to maps on tempered distributions $\mathcal{F}, \mathcal{F}^{-1} : \mathcal{S}'(\mathbb{R}^n) \rightarrow \mathcal{S}'(\mathbb{R}^n)$ and the equations in Proposition 2.2 remain valid.

That $\mathcal{F}, \mathcal{F}^{-1}$ so far defined are truly inverses of each other as maps on $\mathcal{S}(\mathbb{R}^n)$ and $\mathcal{S}'(\mathbb{R}^n)$ is not a priori clear. While we accept the result without proof here, we refer the reader to [2] for its proof.

Stationary Phase Approximation

A useful tool for evaluating oscillatory integrals asymptotically is the method of stationary phase approximation. While we refer the reader to a proof of the derivation of stationary phase approximation in Guillemin and Sternberg [8], we provide a statement of the result here.

Proposition 2.3. *Let $f, g \in C^\infty(\mathbb{R}^n)$ and suppose that g has exponential decay or is compactly supported. Suppose also that there are only finitely many critical points of f in the support of g and that the Hessian $H(f)$ at each of these points is non-degenerate. Then we have*

$$\int g(x) e^{ikf(x)} dx = \left(\frac{2\pi}{k}\right)^{n/2} \sum_{x|df(x)=0} e^{\pi i s \operatorname{sgn}(H(f))/4} \frac{e^{ikf(x)} g(x)}{\sqrt{|\det H(f)|}} + O(k^{-n/2-1}). \quad (2)$$

3 Previous Results

In this section, we state the previously established results essential for our question. While we provide sketches of proofs of the most important of the results, we refer the reader to Hörmander [5] for more rigorous proofs.

Klein-Gordon Equation in Minkowski Spacetime

Theorem 3.1. *Let ψ satisfy equation (1) with $\frac{m^2 c^2}{\hbar^2} = 1$ and suppose that $\psi_0, \psi_1 \in \mathcal{S}(\mathbb{R}^n)$ such that $\psi(0, x) = \psi_0$ and $\partial_t \psi(0, x) = \psi_1$. Then $\psi \in C^\infty(\mathbb{R}_t; \mathcal{S}(\mathbb{R}_x^n))$ and has the form*

$$\psi(t, x) = (2\pi)^{-n} \left(\int_{\mathbb{R}^n} e^{i(x\xi + t\langle \xi \rangle)} \mathcal{F}\psi_{+,0}(\xi) d^n \xi + \int_{\mathbb{R}^n} e^{i(x\xi - t\langle \xi \rangle)} \mathcal{F}\psi_{-,0}(\xi) d^n \xi \right), \quad (3)$$

where $\langle - \rangle$ is the Japanese bracket and

$$\psi_{\pm,0} = \frac{1}{2}(\psi_0 \mp i\langle D_x \rangle \psi_1).$$

Sketch of Proof. We first apply the Fourier transform \mathcal{F} to both sides of equation 1 to get

$$\mathcal{F}\psi = \frac{1}{2}(\mathcal{F}\psi_0(\xi) - i\langle \xi \rangle^{-1} \mathcal{F}\psi_1(\xi))e^{+it\langle \xi \rangle} + \frac{1}{2}(\mathcal{F}\psi_0(\xi) + i\langle \xi \rangle^{-1} \mathcal{F}\psi_1(\xi))e^{-it\langle \xi \rangle}.$$

We see that we may decompose ψ into its “positive and negative frequency parts,” $\psi = \psi_+ + \psi_-$, where $\psi_{\pm} \in \mathcal{S}(\mathbb{R}_x^n)$ are the unique solutions to

$$\partial_t \psi_{\pm} = \pm i\langle D_x \rangle \psi_{\pm}, \quad \psi_{\pm}(0, -) = \psi_{\pm,0}(-),$$

Applying the inverse Fourier transform to ψ_{\pm} gives unique solutions

$$\psi_{\pm}(t, x) = (2\pi)^{-n} \int_{\mathbb{R}^n} e^{i(x\xi \pm t\langle \xi \rangle)} \mathcal{F}\psi_{\pm,0}(\xi) d^n \xi.$$

□

Seeing that ψ_{\pm} have the form of the left hand side of equation (2), it stands that if $x\xi \pm t\langle \xi \rangle$ and $\mathcal{F}\psi_{\pm,0}$ were to satisfy the conditions of Proposition 2.4, we could obtain an asymptotic estimate for ψ . Indeed, $\mathcal{F}\psi_{\pm,0}$ and $x\xi \pm t\langle \xi \rangle$ are smooth and $x\xi \pm t\langle \xi \rangle$ is compactly supported, only having a critical point if $|x| < |t|$, in which case it is given by

$$\xi(t, x) = \mp x \operatorname{sgn}(t)(t^2 - |x|^2)^{-1/2}.$$

Applying Proposition 2.4 then gives us the expansion

$$\psi_{\pm}(t, x) = (1 + o(1))(2\pi)^{-n/2} e^{i\pi n/4} \cdot e^{\pm i\sqrt{t^2 - |x|^2} t^{-n/2}} \cdot \mathcal{F}\psi_{\pm,0}(\xi(t, x)).$$

Assuming that $\mathcal{F}\psi_{\pm,0}(0) = \int_{\mathbb{R}^n} \psi_{\pm,0}(x) d^n(x)$ is nonzero, we arrive at the following conclusion.

Theorem 3.2. *Let ψ be as in equation (3). Then ψ decays like $t^{-n/2}$ as $t \rightarrow \infty$.*

Klein-Gordon Equation with Gravitational Interaction

Extending the Klein-Gordon Equation to general relativity, we must include the effect of gravity by replacing the partial derivatives of the equation with covariant derivatives.

Definition 3.1. Let X be a Lorentzian manifold with metric tensor g in the mostly plus signature. Then the free Klein-Gordon equation is given by

$$\frac{-1}{\sqrt{-\det g}} \partial_\mu (g^{\mu\nu} \sqrt{-\det g} \partial_\nu \psi) + \frac{m^2 c^2}{\hbar^2} \psi = 0, \quad (4)$$

where $g^{\mu\nu}$ is the inverse metric tensor and summation over repeated indices is implied.

Our interest lies in the case of X being Schwarzschild spacetime, the solution of Einstein's field equations describing the gravitational field outside an uncharged, unrotating spherical mass on the assumption that the universal cosmological constant Λ is zero. In this case, g is defined with the Schwarzschild coordinates t , r , θ , and ϕ , and is given by

$$ds^2 = - \left(1 - \frac{2GM}{r} \right) dt^2 + \left(1 - \frac{2GM}{c^2 r} \right)^{-1} dr^2 + r^2 d\theta^2 + r^2 \sin^2 \theta d\phi^2,$$

where G is the gravitational constant, M is the mass of the body, t is the time coordinate measured by a stationary clock located infinitely far away from the body, and r , θ , and ϕ are the standard spherical coordinates representing the radial coordinate, colatitude and longitude, respectively. The quantity $\frac{2GM}{c^2}$ is often denoted by r_s , the Schwarzschild radius, so that g becomes

$$ds^2 = - \left(1 - \frac{r_s}{r} \right) c^2 dt^2 + \left(1 - \frac{r_s}{r} \right)^{-1} dr^2 + r^2 d\theta^2 + r^2 \sin^2 \theta d\phi^2. \quad (5)$$

One observes that the Schwarzschild metric has a singularity at $r = r_s$. Indeed, when $r < r_s$, the space coordinate r becomes timelike while the time coordinate t becomes spacelike. In this regard, the singularity at $r = r_s$ divides the coordinates into two disconnected patches. The use of the above coordinate system thus results in the requirement of two separate analyses for solutions of equations over the spacetime. While this singularity has been shown to be purely a coordinate singularity, we find it more enlightening to use the Schwarzschild coordinates and restrict our analyses to the $r > r_s$ patch.

Combining equations (4) and (5), we arrive at the following.

Proposition 3.3. *The Klein-Gordon equation in Schwarzschild spacetime is given by*

$$\frac{r}{c^2(r-r_s)} \frac{\partial^2 \psi}{\partial t^2} - \frac{1}{r^2} \frac{\partial \psi}{\partial r} \left(r(r-r_s) \frac{\partial \psi}{\partial r} \right) - \frac{1}{r^2 \sin \theta} \frac{\partial \psi}{\partial \theta} \left(\sin \theta \frac{\partial \psi}{\partial \theta} \right) - \frac{1}{r^2 \sin^2 \theta} \frac{\partial^2 \psi}{\partial \phi^2} + \frac{m^2 c^2}{\hbar^2} \psi = 0.$$

In our analyses, we restrict ourselves to spherically symmetric solutions of the Klein-Gordon equation. In this case $\frac{\partial \psi}{\partial \theta} = \frac{\partial \psi}{\partial \phi} = 0$, and so the Klein-Gordon equation becomes

$$\frac{r}{c^2(r-r_s)} \frac{\partial^2 \psi}{\partial t^2} - \frac{1}{r^2} \frac{\partial \psi}{\partial r} \left(r(r-r_s) \frac{\partial \psi}{\partial r} \right) + \frac{m^2 c^2}{\hbar^2} \psi = 0. \quad (6)$$

As the metric structure on X has been perturbed from the metric structure in Minkowski spacetime, the method of applying the Fourier transform to both sides of the Klein-Gordon equation to obtain exact solutions is no longer feasible. One attempt to work around this constraint is to find and analyze numerical solutions of the equation. Since we can make these solutions arbitrarily close to an exact solution, it follows that we could extract asymptotics from these solutions in special cases.

4 Numerical Methods and Partial Results

In spite of analytical difficulties presented when the background space is switched to a Schwarzschild spacetime, we can in theory solve the Klein-Gordon equation numerically in any background space to obtain asymptotics. We used Mathematica's numerical integration and differential equation solving strategies to obtain our solutions. While we found these numerical solutions to be moot at best and erroneous at worst, we present our methods here and relevant code in Appendix A. We also hypothesize our mistakes and describe future numerical strategies to obtain consistent results.

Numerical Asymptotics for the Klein-Gordon Equation in Minkowski Spacetime

Our first task was to validate our numerical methods over known cases. To do this, we compared the asymptotics of the numerical solutions of the Klein-Gordon equation in two-dimensional Minkowski spacetime (one space dimension with time) with those of the solutions described in equation (3). In particular, we tested the case where ψ_0 was an appropriately scaled Gaussian and ψ_1 was set to 0, and compared our results with numerical approximations of ψ_+ in equation (3). Under the assumption that the choice of c was unimportant to our calculation, we let $c = 1$. We also found that for m sufficiently small, singular behavior for ψ occurred asymptotically. To combat this, we set $m = 10$.

We first tested the stability of Mathematica's numerical methods by computing the asymptotic behavior of $|\psi_+|$ using numerical integration. As integration over \mathbb{R}^\times was computationally infeasible, we instead calibrated our initial conditions to be concentrated on the sufficiently small interval $[-1, 1]$ and integrated over that region. Performing a least-squares linear regression on a log-log plot of $|\psi_+(1, t)|$ (see Figure 1) over the time interval $[5000, 20000]$, we arrived at a slope of $-.501$ and an R^2 value of $.9949$. This corresponded to best fit of $t^{-.501}$ for asymptotic decay of $\psi_+(1, t)$ and provided some evidence that Mathematica's algorithms were precise enough for our purposes. We repeated the experiment with $\psi_-(1, t)$ and again found a desirable slope and R^2 value for our log-log scaled linear regression. We did note, however, that when the experiment was repeated for the exact solution $\psi = \psi_+ + \psi_-$, the resulting log-log scaled plot decayed as expected but produced a noisier graph. Noting that the envelope of the solution still decayed desirably, we disregarded this under the assumption that these were results of the oscillatory nature of ψ .

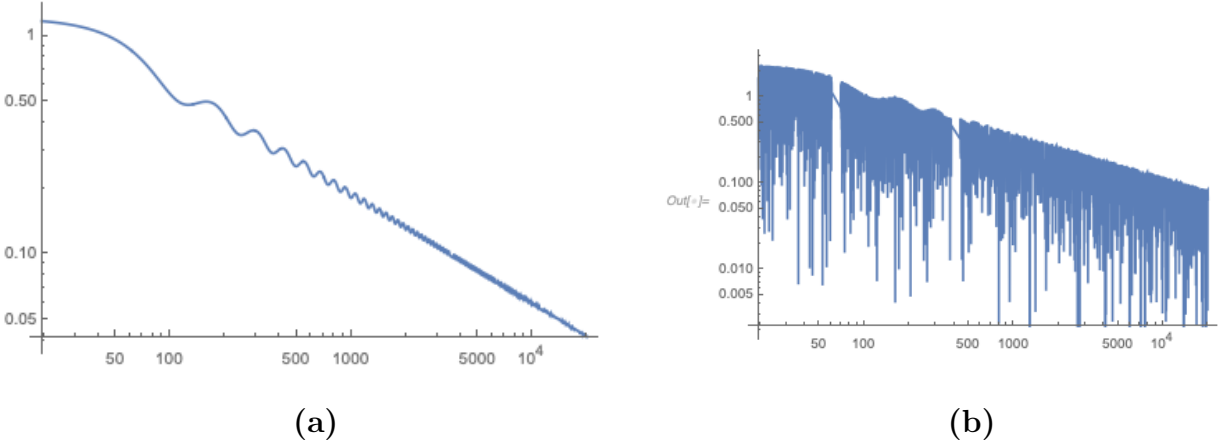


Figure 1: Log-log scaled plots of analytical solutions (a) ψ_+ (b) ψ

After finding that the integration methods of Mathematica were of sufficient stability, we shifted our focus to determining the numerical solution of the Klein-Gordon equation. We solved the equation over the space interval $[0, 10]$, used the same initial conditions as in the integration case, and let $m = 10$ as before. We implemented Neumann boundary conditions for the first time derivative of ψ along the endpoints of our space interval under the assumption that the interval was large enough for the absence of reflectance to be of minimal effect in the asymptotic behavior of ψ .

Solving for ψ over the time interval $[0, 20000]$, we set our space coordinate constant at $x_0 = 5$ and found that $\psi(x_0, t)$ was indeed an oscillatory function that decayed in what appeared to be power law manner before eventually sharply decreasing to machine epsilon. However, the decay to machine epsilon occurred at $t = 1000$, far before the integration case. This marked the first of many disparities between the cases. Taking a log-log plot of $|\psi(x_0, t)|$ over the time interval $[0, 1000]$, we arrived at a plot that was far from linear (see Figure 2). We tried changing c , m , the spread and size of our initial data, the spatial range over which we solved for ψ , and our boundary conditions for this range, but no consistent results were reached. We note that our inability to find any case over which our numerical algorithms worked immediately discredited any coincidental, quasi-consistent results were

we to find them, as it was clear that our methods were unstable in the simplest of cases. Our best guess in this case is that the “Method of Lines” algorithm employed by Mathematica is unstable over large time intervals. For future tests, we would experiment with different solving algorithms and computing systems, while continuing to change boundary conditions.

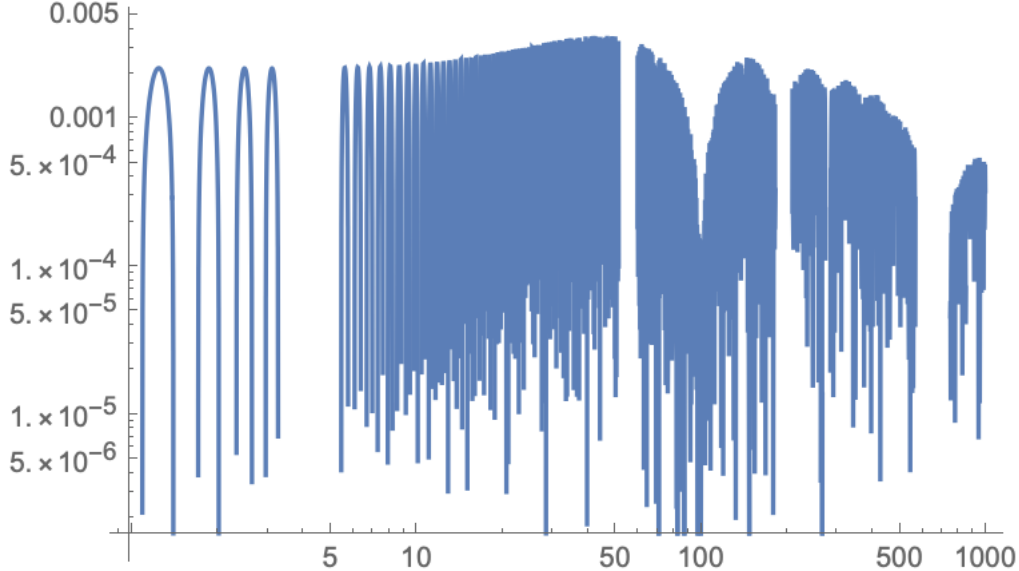


Figure 2: Log-log scaled plot of solution to Klein-Gordon equation in Minkowski spacetime

Numerical Asymptotics for the Klein-Gordon Equation in Schwarzschild Spacetime

While we were not hopeful about the Schwarzschild case giving consistent results after seeing the results obtained in the Minkowski case, we decided to try our methods with the thought that the different metric of Schwarzschild could improve performance. Indeed, considering spherically symmetric solutions to the Klein-Gordon equation in Schwarzschild spacetime, the spatial interval over which we solve the equation has a complete absorbance condition on its left endpoint. We chose this interval to be $[2, 10000]$; the choice of 2 as a left endpoint of the interval avoided the singularity at the origin, and the choice of 10000 as the right endpoint of the interval allowed us to investigate the behavior of ψ when the effect

of asymmetry of the Schwarzschild metric was minimal. We let $x_0 = 5001$, and solved for $\psi(x_0, t)$, where we unsurprisingly failed to attain a linear plot in the log-log scaled graph of $\psi(x_0, t)$. Again, we changed the mass of the system, the initial conditions of the problem, the boundary conditions of the problem, and the space and time intervals over which the problem was solved in hopes of finding some pattern in Mathematica's calculations, though we were unsuccessful in obtaining consistent results on most fronts.

We did find two pieces of interesting information while varying the parameters on our initial value in the Schwarzschild case. The first was that in many of the tests, solutions of the equation failed to have a linear log-log scaled plot in a way dissimilar to how solutions of the equation in the Minkowski case did — the envelope of the log-log plot was bowed out with no change in concavity (see Figure 3). This somewhat indicates that when a stable numerical method is found, it may interpret the Schwarzschild case and Minkowski case differently asymptotically, or that the solutions to the Klein-Gordon equation in these cases are fundamentally different. The second piece of interesting information is that these solutions had the form of Figure 1(b) under a log-linear scaled plot i.e. the envelope of the solutions decayed like e^{-t} . Though more tests must be completed before a formal conjecture is made, we may suspect that $\psi(x, t)$ decays pointwise asymptotically like $\phi(t)e^{-t}$, where $\phi \in \mathcal{S}'(\mathbb{R})$.

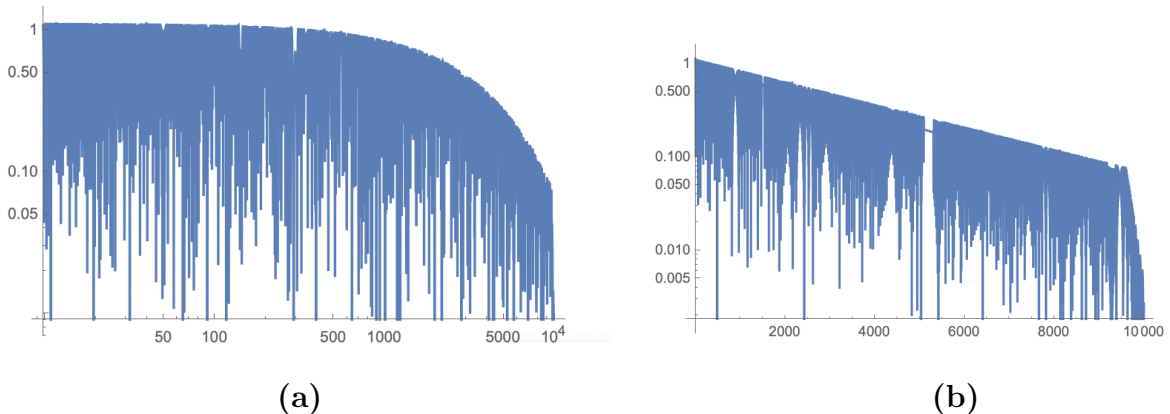


Figure 3: (a) Log-log and (b) Log-linear plots of solution to the Klein-Gordon equation in Schwarzschild spacetime

5 Conclusions

Though we failed to reach numerical results consistent with prior analytical results, we have an indication of which parameters to vary next, and we have greater intuition as to how solutions to the Klein-Gordon equation in Schwarzschild spacetime should behave. When a consistent numerical method is found, the next steps will be to test the stability of the method under varying initial value conditions and dimensions. If in the Schwarzschild case we find that a power law decay does hold, a natural extension to testing our method for non-spherically symmetric solutions with arbitrary Lorentzian manifold background spaces may prove valuable.

6 Acknowledgements

I would like to thank my mentor, Ethan Sussman, of the Department of Mathematics at the Massachusetts Institute of Technology, for his help and guidance with my project, especially considering my late start. I would also like to thank head mentor Dr. Tanya Khovanova of MIT for helping me drastically improve my writing abilities. I would like to thank my tutor, Dr. John Rickert, for helping me edit and formalize this project. I also give my thanks to Professors David Jerison and Ankur Moitra of MIT for their useful ideas and advice. I offer my thanks to Rupert Li and Boris Zbarsky for their useful edits. I would also like to thank Dr. Slava Gerovitch of MIT and Dr. Amy Sillman for organizing the math portion of RSI and helping to quickly find my mentor after a sudden displacement in mentorship. I would also like to thank the Center for Excellence in Education for giving me the opportunity to attend Research Science Institute, and MIT for its generosity in allowing us to use its resources. Finally, I would like to thank my sponsors, who made my experience at RSI possible.

References

- [1] E. Schrödinger. An undulatory theory of the mechanics of atoms and molecules. *Physical review*, 28(6):1049, 1926.
- [2] M. Reed. *Methods of modern mathematical physics: Functional analysis*. Elsevier, 2012.
- [3] J.-M. Lévy-Leblond. Nonrelativistic particles and wave equations. *Communications in Mathematical Physics*, 6(4):286–311, 1967.
- [4] O. Klein. Quantentheorie und fünfdimensionale relativitätstheorie. *Zeitschrift für Physik*, 37(12):895–906, 1926.
- [5] L. Hörmander. *Lectures on nonlinear hyperbolic differential equations*, volume 26. Springer Science & Business Media, 1997.
- [6] L. M. Burko and G. Khanna. Universality of massive scalar field late-time tails in black-hole spacetimes. *Physical Review D*, 70(4):044018, 2004.
- [7] M. do Carmo. *Riemannian Geometry*. Mathematics (Boston, Mass.). Birkhäuser, 1992.
- [8] V. Guillemin and S. Sternberg. *Geometric asymptotics*. Number 14. American Mathematical Soc., 1990.

A Mathematica Code

Code for Analytical Solution of Klein-Gordon Equation in Minkowski Spacetime

```
ClearSystemCache[];
ClearAll[x, t];
m = 10;

Monitor[
  LogLogPlot[
    Abs[NIntegrate[Exp[I ((1 - y) p + t Sqrt[m^2 + p^2])] * Exp[-(y^2)] / 2 +
      Exp[I ((1 - y) p - t Sqrt[m^2 + p^2])] * Exp[-(y^2)] / 2, {y, -1, 1}, {p, -1, 1},
      MaxRecursion -> 20, AccuracyGoal -> 4, Method -> {Automatic, "SymbolicProcessing" -> 0}], {t, 0, 20000}],
    ProgressIndicator[t, {0, 20000}]]
```

Code for Finding Numerical Solutions of the Klein-Gordon Equation in Minkowski Spacetime

```
eqn = D[u[t, x], {t, 2}] + 100 * u[t, x] ==
  D[u[t, x], {x, 2}] + NeumannValue[-Derivative[1, 0][u][t, x], x == 0 || x == 10];
u0[x_] := Evaluate[D[1.25 Erf[(x - 5) / 1.25], x]];
ic = {u[0, x] == u0[x], Derivative[1, 0][u][0, x] == 0};
ufun = NDSolveValue[{eqn, ic}, u, {t, 0, 20000}, {x, 0, 10},
  Method -> {"MethodOfLines", "SpatialDiscretization" -> {"FiniteElement"}}];
```

Code for Finding Numerical Solutions of the Klein-Gordon Equation in Schwarzschild Spacetime

```
eqn = ((x - 1) / x) * D[u[t, x], {t, 2}] + 100 * u[t, x] ==
  1 (1 / x^2) * D[(x) * (x - 1) * D[u[t, x], x], x] +
  NeumannValue[-Derivative[1, 0][u][t, x], x == 2 || x == 10000];
u0[x_] := Evaluate[D[2000 Erf[(x - 5001) / 2000], x]];
ic = {u[0, x] == u0[x], Derivative[1, 0][u][0, x] == 0};
ufun = NDSolveValue[{eqn, ic}, u, {t, 0, 500000}, {x, 2, 10000},
  Method -> {"MethodOfLines", "SpatialDiscretization" -> {"FiniteElement"}}];
Plot[Abs[ufun[t, 5001]], {t, 0, 150000}, ScalingFunctions -> {"Log", "Log"}]
```